Cement and Concrete Research 39 (2009) 580–589

Contents lists available at ScienceDirect

Cement and Concrete Research

journal homepage: http://ees.elsevier.com/CEMCON/default.asp

Mechanism of stabilization of Na-montmorillonite clay with cement kiln dust

Sulapha Peethamparan [a,*], Jan Olek [b], Sidney Diamond [c]

[a] Department of Civil & Env. Eng., 8 Clarkson Avenue, Clarkson University, NY 13699, USA
[b] School of Civil Engineering, Purdue University, 550 Stadium Mall Drive, West Lafayette, IN. 47907-2051, USA
[c] Emeritus, Purdue University, 550 Stadium Mall Drive, West Lafayette, IN. 47907-2051, USA

ARTICLE INFO

Article history:
Received 29 January 2008
Accepted 27 March 2009

Keywords:
Cement kiln dust
Montmorillonite clay
Stabilization
Mechanism
Microstructure

ABSTRACT

A study of the physicochemical interaction of a high free lime (CaO) content cement kiln dust (CKD) with expansive Na-montmorillonite clay is presented. Moist compacted specimens of the CKD-treated clay, the clay alone, the CKD alone, and (for comparison) the clay treated with 7% CaO were each cured for periods up to 90 days and examined by XRD, TGA, and SEM techniques. The results for the CKD-treated clay indicated that calcium hydroxide, derived from the CaO present in the CKD, was extensively adsorbed on the surfaces of the clay flakes, but apparently only limited pozzolanic reaction occurred. Gypsum was rapidly produced from sulfate-bearing components in the CKD, and subsequently ettringite was produced as well, some of the latter apparently incorporating aluminum derived from the clay. Much of the clay was left unreacted, but the morphology of the clay particle assemblage was significantly modified in response to the CKD treatment. Similar morphological changes were also induced by the CaO treatment, suggesting that similar underlying mechanisms were also active here.

1. Introduction

Cement kiln dust (CKD) is a finely-divided particulate material carried in the air stream of a cement kiln and removed by the plant's air pollution control system. In essence, any given CKD is a mixture of airborne particles of cement-making raw materials, partly-processed cement grains, and volatile components condensed on their surfaces. CKDs generated by different plants vary in composition, but most of them contain quartz, calcium carbonate, and calcium oxide (CaO or "free lime"); many also contain alkali sulfates, chlorides and other minor components. The relative proportions of these components are highly variable. Most CKDs tend to generate relatively highly alkaline pH levels when mixed with water. The major existing application of these CKDs is for soil stabilization [1–6], although a variety of minor applications have also been developed [7–18].

Recently, the authors of the current paper focused on investigations of the effectiveness of several different CKDs as soil stabilizers for kaolinite [19] and for Na-montmorillonite [20] clays. The results of these studies indicated that when compacted, CKD-treated kaolinite and Na-montmorillonite clays both developed substantially increased compressive strengths compared to those of the respective untreated clays, with the degree of improvement increasing both with the amount of CKD and with the duration of curing. It was also found that CKDs with higher free lime content were more effective in enhancing strength, and also in lowering the swelling potential and in reducing the plasticity index of the Na-montmorillonite clay [20].

In the present paper, the authors provide the results of investigations aimed at understanding the mechanisms responsible for CKD-induced improvements in properties of the expansive Na-montmorillonite clay. The mechanism of CKD-induced improvements in properties of non-expansive kaolinite clay has been described elsewhere [21]. In the present study a single, highly reactive CKD was used, and the interactions between this CKD and the Na-montmorillonite clay were followed over a 90-day moist curing period, using X-ray diffraction (XRD), thermogravimetric analysis (TGA) and scanning electron microscopy (SEM) including energy-dispersive X-ray spectroscopy (EDX). Specimens produced by combining this CKD alone with water were also studied, in order to distinguish these reaction products from those formed in the presence of clay. A parallel study of the effects of quicklime addition on the clay properties was also carried out, since some details of lime–clay interactions have long remained unresolved [22,23].

2. Raw materials, test specimens and experimental details

2.1. Raw materials

The raw materials used in this study included unreacted (dry) CKD powder, dry Na-montmorillonite clay, and reagent grade unhydrated CaO (quicklime). The pertinent chemical and physical characteristics of these materials are presented below.

* Corresponding author. Tel.: +1 315 268 4435.
E-mail address: speetham@clarkson.edu (S. Peethamparan).

0008-8846/$ – see front matter © 2009 Elsevier Ltd. All rights reserved.
doi:10.1016/j.cemconres.2009.03.013

2.1.1. CKD powder

The particular CKD used in the present study was a relatively coarse CKD, collected from a dry-process plant equipped with a precalciner and a short kiln. When mixed with water, this CKD produced a highly alkaline pH of 13.2, which was substantially greater than the pH 12.5 that is produced by CaO or $Ca(OH)_2$. The kiln feed used in this plant included limestone, clay, bottom ash, fly ash, foundry sand, sludge and iron waste. The overall chemical composition of this CKD is given in Table 1, which (for comparative purposes) also provides the chemical composition of a typical Type I Portland cement; both being obtained by X-ray fluorescence (XRF) spectroscopy. It can be seen that this particular CKD contains a somewhat lower content of analytical CaO than the finished Portland cement (55% vs. ~63%), a much higher analytical SO_3 content (~13% vs. 2.5%); and a higher alkali content (~2% vs. ~0.4% equiv. Na_2O). In addition, the content of actual free lime (uncombined CaO) is very much greater in the CKD (~29%) than in the cement (~1.6%). It should be noted that the free lime content was determined using a method that involved dissolution of CaO in ethylene glycol followed by titration with the benzoic acid; such a procedure is considered accurate but it is not one of the standardized methods.

Fig. 1 provides the XRD pattern obtained for the original CKD powder. The pattern is obviously dominated by the characteristic peaks for uncombined CaO (free lime). Other crystalline components detected include anhydrite ($CaSO_4$), small amounts of calcite ($CaCO_3$), arcanite (K_2SO_4), and quartz (SiO_2). No XRD peaks for cement minerals were detected. It should be reiterated that different CKDs can vary widely in composition and, as a result, the composition of this CKD should not be considered characteristic of CKDs in general. More detailed presentation of the range of components found in various CKDs was provided by Peethamparan et al. in another publication [24].

The specific surface area of this CKD powder was measured by the nitrogen BET method and was found to be 1.8 m^2/g. Laser particle size analysis indicated a mean particle size of approximately 30 μm, but scanning electron microscopy (SEM) examination suggests that most of the "particles" were in fact undispersed or cemented agglomerations. Fig. 2 provides a view of a typical group of such particles, and also includes several recognizable fly ash spheres.

2.1.2. Dry Na-montmorillonite clay

The clay used in this study was a commercial sodium Wyoming bentonite, marketed as Volclay™ by the American Colloid Company. For brevity we will subsequently refer to this Na-montmorillonite clay as "Na-m clay". Its specific surface area was measured as 27 m^2/g using nitrogen BET, but 600 m^2/g using the EGMA (ethylene glycol monoethyl ether) method [25]. The latter method records both, the interlayer surfaces as well as the external surfaces of the particles.

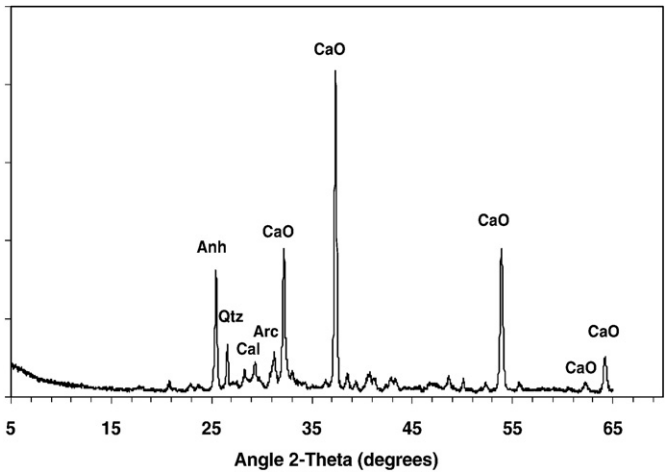

Fig. 1. XRD pattern for the CKD powder: Anh—anhydrite, Qtz—quartz, Arc—arcanite, CaO—calcium oxide, Cal—calcite.

The XRD pattern (CuKα radiation) for this as-received clay (not presented) showed the typical basal montmorillonite peak at 2θ angle of about 7°. The major impurity visible in the pattern was quartz, but there was also a small XRD peak for gypsum.

The measured Atterberg limits of this highly expansive clay were: liquid limit: 444% and plastic limit: 40%, yielding a very high plasticity index of slightly more than 400%.

2.1.3. Unhydrated lime

Analytical reagent grade CaO was used in preparation of lime–clay mixtures. The nomenclature of calcium oxides and hydroxides is often a subject of confusion. In this paper, we refer to this reagent grade CaO simply as "lime", to distinguish it from the uncombined CaO present as the major component in the CKD, which will be referred to as "free lime". Calcium hydroxide and calcium carbonate (both of which are also sometimes called lime) will be referred to by their respective chemical designations.

2.2. Test specimens

The specimens studied in this work were prepared in the form of small compacted cylinders, 33 mm in diameter and 71 mm in height, using the Harvard miniature compaction apparatus [26]. This device

Table 1
Chemical analyses of the CKD, of a typical Type I Portland cement and of the Na-montmorillonite (Na-m).

Chemical composition	CKD	Type I	Na-m
	Weight (%)		
SiO_2	16.42	20.48	63.02
Al_2O_3	3.62	4.21	21.08
TiO_2	0.23	0.36	–
P_2O_5	0.09	0.09	–
Fe_2O_3	2.31	2.41	3.25
CaO	55.00	63.19	0.65
MgO	2.68	4	2.67
Na_2O	0.17	0.19	2.57
K_2O	2.89	0.28	–
Na_2O equiv.	2.05	0.37	
Mn_2O_3	0.44	0.14	
SrO	0.03	0.04	
SO_3	12.69	2.76	
Cl	0.74	–	
LOI@ 750	3.92	1.76	
Free CaO	29.14	1.58	

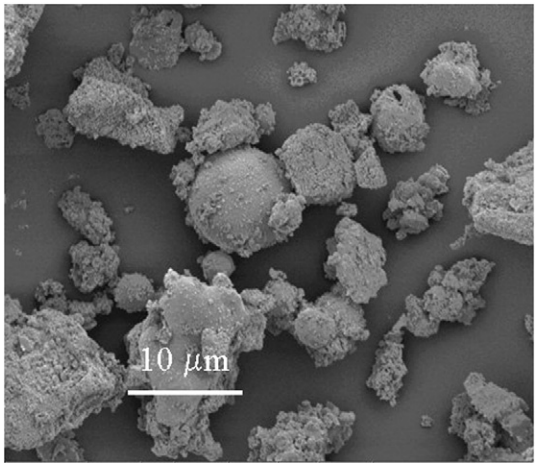

Fig. 2. CKD "particles" as observed in scanning electron microscope.

uses a compaction method that closely duplicates the kneading action of the sheeps-foot roller used in soil compaction, but requires only about 200 g of moist soil or soil mixtures.

Four sets of moist-compacted specimens were prepared. These were respectively: (1) the Na-m clay, (2) the CKD, (3) the CKD-treated Na-m clay (mixed at a proportion of 25% CKD by weight of the clay) and (4) lime-treated Na-m clay, mixed at a proportion of 7% of lime by weight of the clay. All of the specimens, except the CKD alone samples, were compacted at the identical moisture content of 38% (approximately the optimum moisture content of the clay) by weight of the dry components. The CKD alone samples were compacted at a moisture content of 31%. The percentage of lime in the lime-treated Na-m clay was selected as being the same as the content of free lime in the 25% CKD-treated Na-m clay, thus providing comparison of the two systems both containing the same free lime (CaO) content.

When preparing the "Na-m clay" and the "CKD" test specimens, the distilled water was added directly to the dry powders in the amount required to bring them to the designated 38% moisture content. In preparing the "CKD-treated Na-m clay and "lime-treated Na-m clay" specimens, the two dry components were first combined (on a weight basis) and homogenized by mixing them in a reciprocating paint shaker for 15 min, after which distilled water was added to bring the resulting mixture to the specified 38% moisture content. For each set of test specimens, the wetted powders were then compacted into the steel molds of the Harvard Miniature Compaction device, using the standardized procedure described in USBR-Standard 5510 [26]. The compacted cylinders were extracted immediately after compaction, wrapped in plastic bags, placed in sealed plastic boxes and stored in a room kept at 100% RH at a constant temperature of 23 °C. After designated curing periods of 1, 7, 28 and 90 days, small (10 mm) cubic specimens were cut from the cylinders and then freeze-dried to remove the water without undue distortion of the existing microstructure. The freezing was performed by dipping the sample in liquid nitrogen for several seconds. This was followed by drying under vacuum at room temperature for one day, a process that removes most, but not necessarily all of the uncombined water. After one day of drying, the small cube specimens were placed in airtight glass vials which were stored in desiccators until required for testing.

2.3. Details of the investigation of compacted test specimens

2.3.1. X-ray diffraction analyses

Randomly oriented powder specimens for XRD analysis were prepared by grinding small portions of the freeze-dried specimens and sieving the ground material through a 200-mesh sieve. The XRD was carried out using a Siemens D-500 diffractometer using CuKα radiation at 50 kV and 30 mA, scanning being carried out from 3° to 65° 2θ, at 0.02° intervals.

2.3.2. Thermogravimetric analyses

TGA was performed using a TA 2950 thermogravimetric analyzer, using representative 30 mg powdered samples prepared as discussed in Section 2.3.1 above, without further pre-conditioning. The powdered samples were continuously heated in a flowing nitrogen environment at a heating rate of 10 °C/min. from room temperature to 1000 °C. Both TGA and differential TGA (DTGA) patterns were obtained.

2.3.3. Scanning electron microscopy

Freeze-dried, cube-shaped specimens prepared as described earlier were fractured to expose clean fresh surfaces. The specimens were then mounted on aluminum stubs using carbon tape and silver paint, and the exposed fractured surfaces were sputter-coated with platinum. SEM examination was carried out on these fractured surfaces in the secondary electron mode. An FEI NOVA nanoSEM field emission SEM operated at 15 keV was used, with either an Everhart-Thornley detector or a through-the-lens detector. Energy-dispersive X-ray (EDX) analyses were obtained at selected locations using an Oxford INCA 250 EDX system.

3. Experimental results and analysis

3.1. Compacted Na-m clay

The TGA and DTGA curves obtained for the moist-compacted Na-m clay are given in Fig. 3. The weight loss between 80 °C and 105 °C is primarily due to the loss of adsorbed water from the clay; the second major weight loss at ~700 °C is due to dehydroxylation of OH, i.e., the loss of structural OH groups which combine and are emitted as water molecules. The small peak at 110 °C is apparently due to decomposition of the impurity gypsum present in the clay.

A typical SEM micrograph obtained from the moist-compacted Na-m clay is shown in Fig. 4, along with a typical EDX spectrum. The fractured surface reveals an assemblage of undulating filmy particles. While the outlines of particles raised above the general fracture surface are quite sharp, the outlines of individual particles blending into the mass are not easy to detect. Montmorillonite particles are frequently described and diagrammed as very thin plates; it is clear that the actual particles in this compacted montmorillonite are very thin, but far from platy.

EDX spectra were secured at various locations, a representative one being included in Fig. 4. It shows major peaks for oxygen, aluminum and silicon, smaller peaks for sodium and magnesium, and traces of the presence of sulfur. The Si:Al peak height ratio is approximately 2:1, as expected for montmorillonite. Somewhat surprisingly, no discernable quartz grains were detected on the fracture surface despite the presence of appreciable quartz impurity in the XRD pattern.

It was found that the unconfined compressive strength developed by the moist-compacted Na-m clay specimens was quite modest, the value being approximately 400 kPa at one day; it did not change appreciably with curing.

3.2. Compacted CKD specimens (without clay) and effects of curing time

The XRD patterns for CKD specimens compacted with 31% of water and cured for periods of time varying from 1 to 90 days is shown in Fig. 5. Note that for ease of comparison, the XRD pattern of the dry CKD powder previously shown in Fig. 1 has also been included in Fig. 5. It can be seen that shortly after water addition almost all of the CaO (free lime) originally present in the CKD powder was converted to calcium hydroxide (CH), which thus became a major component. Anhydrite, present at early ages, was replaced by ettringite, gypsum and syngenite on further curing. These results were confirmed by DTGA analyses (not reported here but published elsewhere [24]), which showed peaks for the ettringite and gypsum at later ages. Both

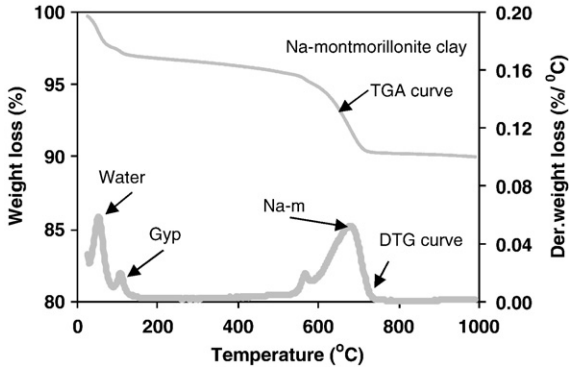

Fig. 3. TGA and DTGA patterns for the moist-compacted Na-m clay.

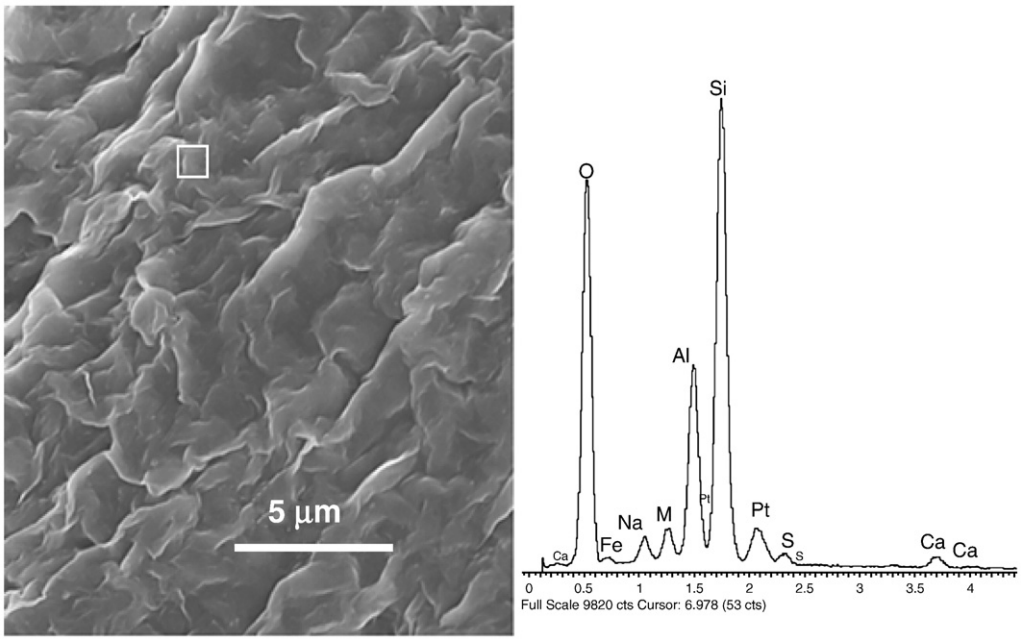

Fig. 4. SEM micrograph of a fracture surface of moist-compacted Na-m clay (left) and typical EDX spectrum. The platinum detected is from the conductive coating applied to the surface of the specimen.

the XRD and DTGA peaks for ettringite increased progressively with curing.

As would be expected from its high free lime content, this CKD is highly self-cementing. The unconfined compressive strength of the material compacted with 31% water was about 1300 kPa at one day; it increased with curing to about 9000 kPa at 90 days [24].

A representative SEM micrograph of the freeze-dried compacted CKD specimen that had been cured for 28 days is presented in Fig. 6. Platy crystals of calcium hydroxide (CH), needle-shaped particles that are presumably ettringite (E), and variously-shaped syngenite crystals (S) were found, along with what appeared to be cemented fine particles containing calcium, silica, and sulfur and indicated as "C–S–H?". These

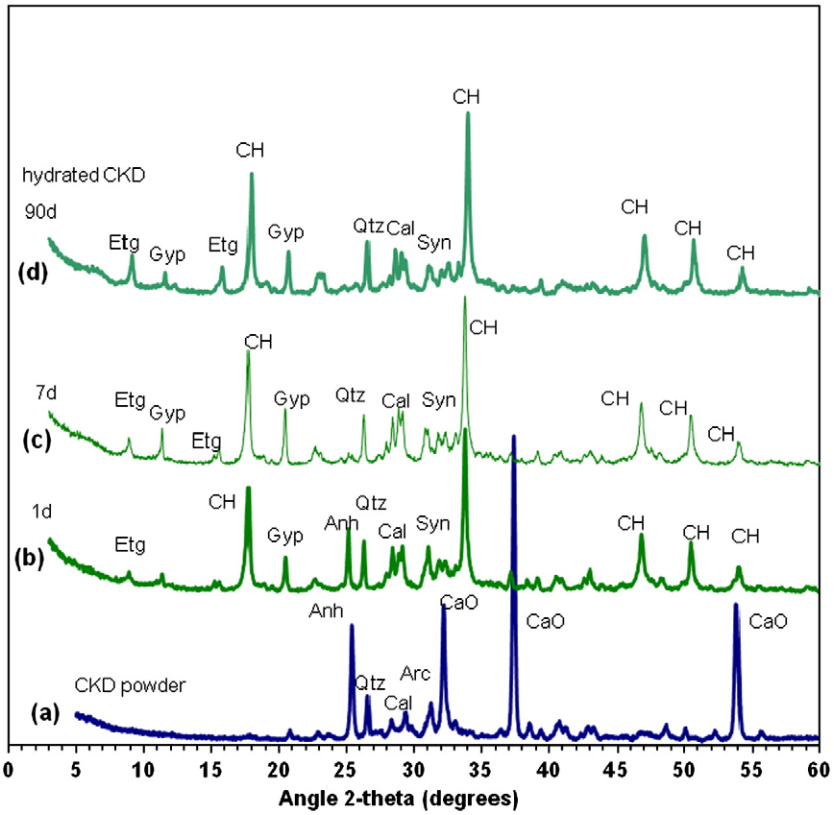

Fig. 5. X-ray patterns of (a) dry CKD powder and ((b)–(d) compacted CKD specimens cured for various periods (Etg—ettringite, Gyp—gypsum, Cal—calcite, Qtz—quartz, Syn—syngenite, CH—calcium hydroxide, Anh—anhydrite, CaO—calcium oxide, Qtz—quartz, Arc—arcanite, Cal—calcite).

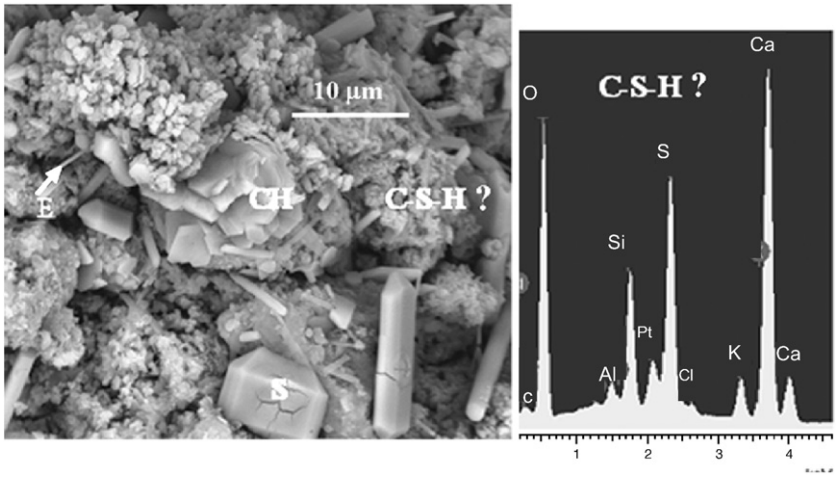

Fig. 6. Area in a compacted CKD specimen cured for 28 days. Note platy calcium hydroxide (CH) crystals, syngenite (S) crystals, and thin needle-shaped ettringite (E) crystals. The fine textured material designated "C–S–H?" has the Ca–S–Si composition indicated by the EDX spectrum.

particles resembled calcium silicate hydrate somewhat in appearance, but wherever found, they incorporated large contents of sulfate and some potassium as well as Ca and Si. No areas were found in the specimen that showed "normal" EDX C–S–H spectra.

3.3. Compacted lime-treated Na-m clay, and effects of curing time

XRD patterns of the freeze-dried 90-day old, moist-compacted Na-m clay specimen and of 7% lime-treated Na-m specimens cured for various lengths of time are all shown in Fig. 7. The XRD patterns for as-received clay (not shown) were very similar to that of the freeze-dried compacted specimen. Curing did not change the XRD pattern of the moist-compacted specimen of the Na-m specimen, and therefore earlier pattern is not shown here.

Only a trace of calcium hydroxide was found in the lime-treated clay specimens, and this was only found for the first week. No XRD indication for C–S–H was found at any age; however, small contents of C–S–H are not generally possible to detect by XRD, and even when it exists in major proportions, detection of this quasi-amorphous phase is often ambiguous.

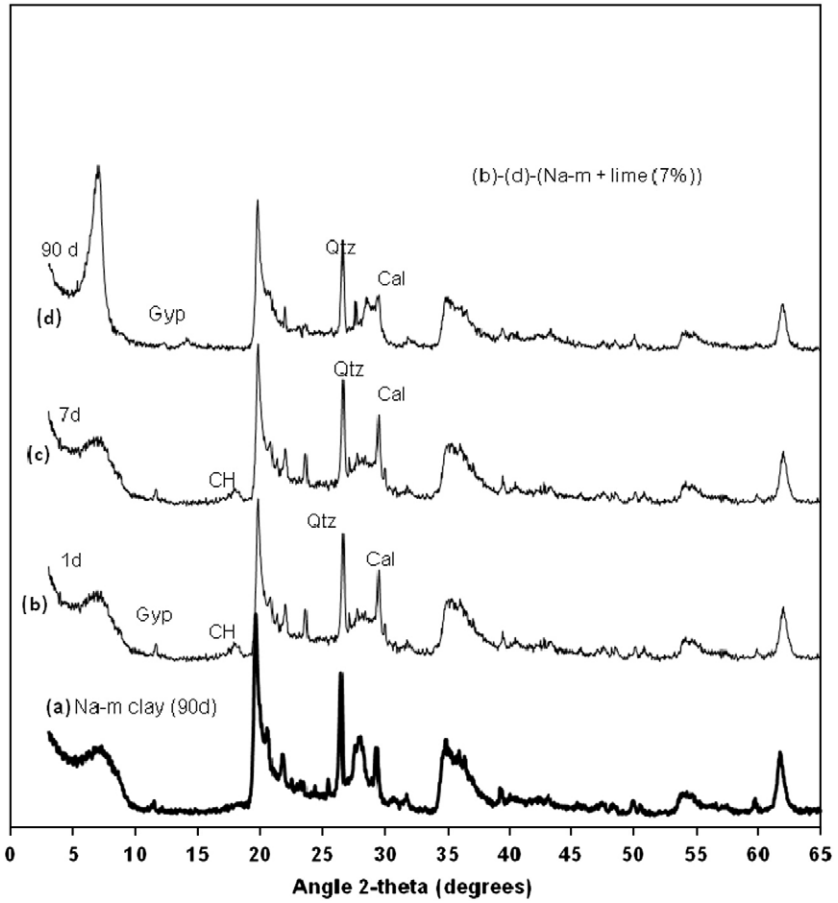

Fig. 7. X-ray patterns of 28 days old moist-compacted (a) untreated Na-m clay and ((b)–(d)) lime-treated Na-m clay at different curing periods: Gyp—gypsum, CH—calcium hydroxide, Qtz—quartz, Cal—calcite, Na-m—Na-montmorillonite clay.

The basal peak for the montmorillonite (at about 7° 2θ) was seen to sharpen noticeably between 7 and 90 days, and to shift to a slightly lower 2θ position. Otherwise, the XRD pattern for the montmorillonite seemed to be generally unaffected by the CaO treatment.

The TGA and DTGA results for the original clay and for the lime-treated clay specimens are shown in Fig. 8. The DTGA peak for the dehydroxylation of the montmorillonite near 700 °C (marked as Na-m dehy.) appears to be much smaller for the lime-treated clays than what would be expected simply by dilution of the clay with 7% lime. This feature seems to be associated with gradual weight loss between about 200 °C and about 600 °C seen in the corresponding TGA curves.

In contrast, the low temperature peak (near 100 °C) increases significantly in amplitude with curing. This increase may be associated with increases in the absorbed water retained by the freeze-dried specimens, or with formation of C–S–H, although the latter has not been detected. Possible interpretations of these observations are provided in the "Discussion" section of this paper.

A representative SEM micrograph for the lime-treated Na-m clay after 90 days of curing is shown in Fig. 9, along with EDX spectra taken at locations marked "A" and "B".

The undulating and film-like appearance of the original Na-m particles seen previously in Fig. 4 is no longer evident. The EDX spectra taken at locations marked "A" and "B" both show relatively strong Ca peaks, in addition to the Si and Al peaks of the clay. Similar evidence for the presence of significant amounts of calcium was found at all locations examined.

Despite this incorporation of calcium throughout the lime-treated clay and its changed morphological appearance, the XRD results suggest that extensive chemical reaction did not appear to take place.

3.4. Compacted, CKD-treated Na-m clay and the effects of curing time

The 25% CKD-treated Na-m clay appeared to be reasonably well stabilized since its unconfined compressive strength progressively increased from 1000 kPa at 1 day to approximately 2400 kPa at 90 days, values much greater than the 400 kPa strength of the compacted clay alone [20].

Fig. 10 shows XRD patterns of the clay treated with CKD and cured for 1, 7, 28 and 90 days, in addition to the XRD pattern for 28 day-old Na-m clay by itself. The montmorillonite basal peak in the CKD-treated clay remained sharply defined, and it showed no appreciable change in intensity or position with progressive curing. Similarly to what was shown in Fig. 7 for the lime-treated clay, no XRD indication of the formation of C–S–H was found even at later ages. In the

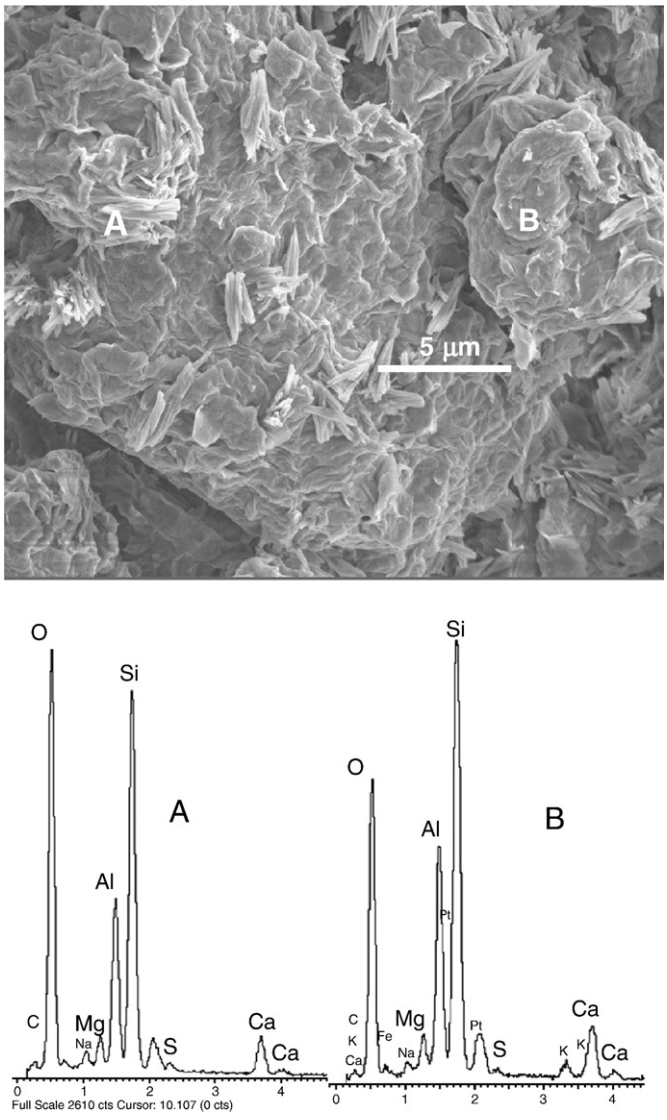

Fig. 9. SEM micrographs of lime-treated Na-montmorillonite clay after 90 days curing, showing large aggregates of the clay flakes (top) and the EDX spectra collected at two positions marked "A" and "B" (bottom).

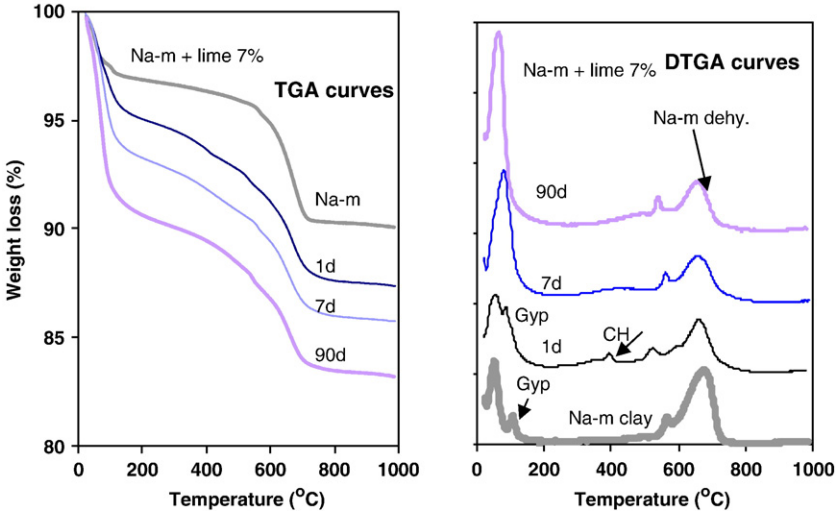

Fig. 8. Thermogravimetric analyses of lime-treated Na-montmorillonite at various curing periods (C–S–H—calcium silicate hydrate, CH—calcium hydroxide, G—gypsum, Cal—calcite).

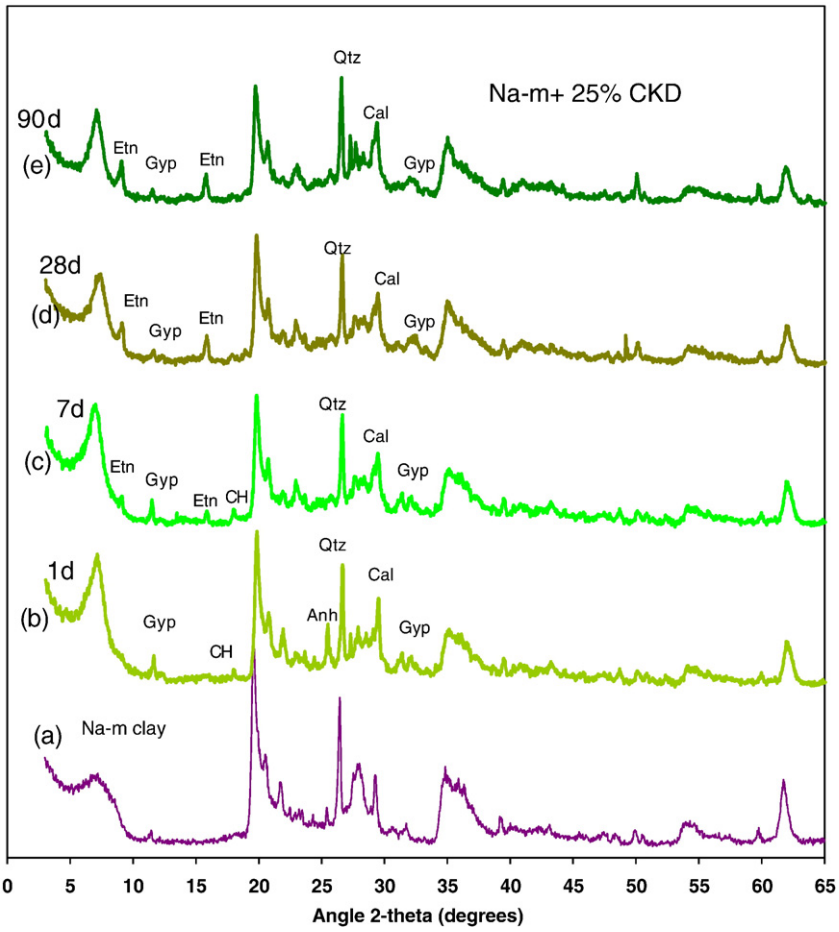

Fig. 10. X-ray patterns of the (a) Na-m and the ((b)–(e)) CKD-treated Na-m at different curing periods (Etn—ettringite, CH—calcium hydroxide, Anh—anhydrite, Gyp—gypsum, Qtz—quartz, Cal—calcite, Na-m—sodium montmorillonite clay).

presence of the clay, the XRD peaks for CH completely disappeared by 90 days of curing, despite the fact that this component developed into a major peak when the CKD was hydrated without clay being present (see Fig. 5). It was noted that some anhydrite from the CKD was retained in the 1 day pattern, but it disappeared completely thereafter. A trace of the gypsum peak persisted, but it is clear that the XRD peaks attributed to ettringite increased between 7 and 90 days.

The TGA analyses results of both CKD-treated and untreated Na-m clay are shown in Fig. 11. They closely resemble those of Fig. 8 for the CaO–Na-montmorillonite specimens. There was a clear and progressive increase in the height of the low temperature DTGA peak with curing, as there was in Fig. 8. Also, as in Fig. 8, the DTGA dehydroxylation peak near 700 °C was substantially smaller in the CKD-treated specimens than in the untreated clay and the TGA pattern

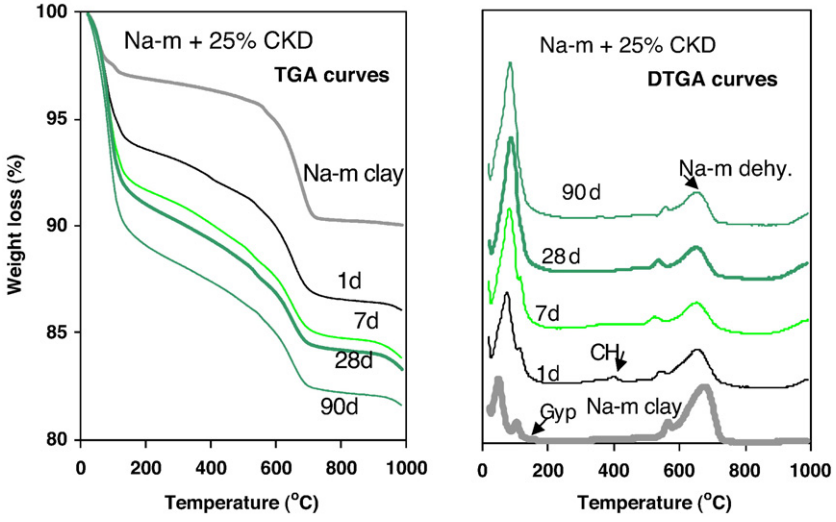

Fig. 11. Thermogravimetric analysis of compacted untreated and CKD-treated Na-montmorillonite clay at various curing periods (Etn—ettringite, CH—calcium hydroxide, Gyp—gypsum, C–S–H—calcium silicate hydrate).

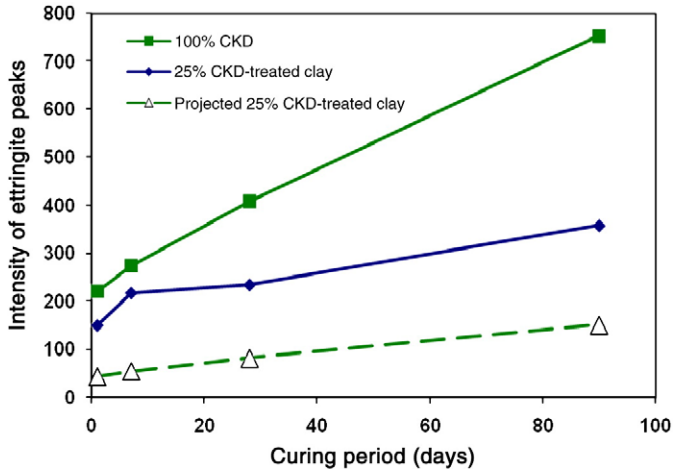

Fig. 12. Intensity of ettringite XRD peaks in compacted CKD alone, in compacted CKD-treated Na-m clay, and the projected ettringite peak height expected in the CKD-treated Na-m clay on the basis of proportionality.

showed significant, but gradual, weight loss between about 200 °C and about 600 °C. Further interpretation of these features will be considered in the "Discussion" section.

It is of interest here to try to map the intensities of the XRD peak ascribed to ettringite in the CKD–Na-m specimens and in the corresponding CKD specimens without clay. The data are provided

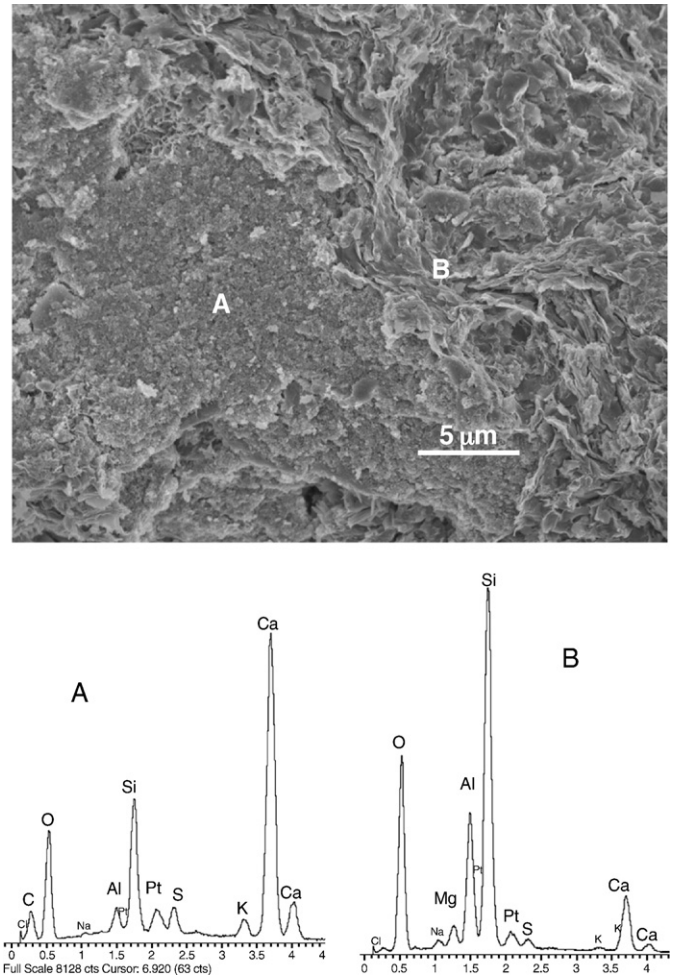

Fig. 13. SEM micrograph of CKD-treated Na-m specimen cured for 90 days, with EDX spectra for locations marked "A" and "B".

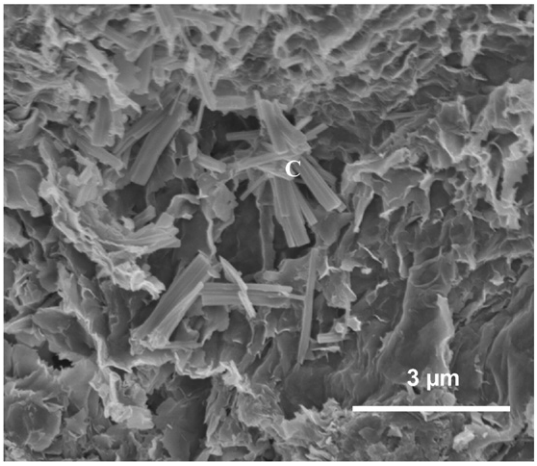

Fig. 14. Cluster of elongated particles found in CKD-treated Na-m clay cured for 90 days.

in Fig. 12. The same figure also shows the ettringite peak intensities expected if the effect of incorporating the clay was only that of dilution of the CKD, i.e. that the presence of the clay did not influence the generation of ettringite from the CKD. It appears that the amount of ettringite found in the CKD-treated clay specimens at any age is about twice that expected on the basis of the proportion of CKD present. Thus, it appears that additional ettringite may have been formed, presumably by incorporating alumina liberated from the clay.

SEM investigation of the CKD treated Na-m specimens disclosed that significant microstructural changes were induced by the incorporation of the CKD, but that these changes were not quite the same as those found with the lime-treated clay. Fig. 13 shows an area of the fractured surface of the CKD-treated clay after 90 days of curing, along with EDX spectra taken at two locations (A and B). The fractured surface clearly shows the presence of agglomerates rather than individual flakes, as did Fig. 9 for the lime-treated clay. In many areas, the EDX spectra show the expected clay components with only a small content of Ca, as did the lime-treated clay (see spectrum for location, "B").

On the other hand, the microstructure around the location marked "A" is quite different. The microstructure of this agglomeration of particles is very much denser and finer-textured than the clay microstructure around "B". Its EDX spectrum is also very different; showing Ca and Si as the major constituents with an apparent Ca/Si ratio of ~2. Small peaks for aluminum and sulfur were also present. Such compositions are characteristic for C–S–H formed in cement-based materials. It appears therefore that this dense local region represents C–S–H reaction product.

It is recalled (see Fig. 10) that XRD peaks for ettringite were recorded in the more mature CKD-Na-montmorillonite specimens. We found small contents of elongated particles in local areas on the fractured surfaces of CKD-treated clay, as seen for example in Fig. 14. In some areas the elongated particles appeared to be more densely intergrown with the clay.

Because of the thinness of the elongated particles, which were only about 0.3 µm thick, it was not possible to get an EDX spectrum that did not also reflect the composition of the surrounding aluminosilicate clay. Nevertheless, it appears that these elongated particles represent the ettringite found in the specimen by XRD.

4. Discussion

It has been shown that incorporation of the cement kiln dust induced extensive changes in the physico-chemical properties of Na-montmorillonite clay. The strength of CKD-treated and moist-compacted Na-m clay specimens increased substantially even after one day, and progressively with further curing [20]. It was also noted

in the previous study [20] that pH of the CKD–clay system was initially quite high (~13) but by 7 days of curing it had dropped to 12.5, the value characteristic of saturated calcium hydroxide solution. This 12.5 pH value was maintained at later ages, despite the disappearance of crystalline calcium hydroxide from the XRD spectrum and from the DTGA pattern.

The SEM observations revealed that calcium appeared in the EDX spectra displayed for essentially all portions of the fractured surfaces of the CKD-treated clay. It thus appears that the calcium hydroxide generated by the CKD was adsorbed fairly quickly on the clay surfaces. It further appears that the absorbed calcium hydroxide was capable of maintaining the pH of a saturated calcium hydroxide solution.

As described earlier, the DTGA analyses show progressively stronger dehydration peaks (at around 100 °C) with curing in both lime-treated and CKD-treated specimens. A number of reasons might be postulated for this effect. In the CKD-treated specimens the progressive increase in ettringite content, as shown by XRD in Fig. 10, may be partly responsible, but this is not so for the lime-treated specimens. A second possible contributing factor might be increased contents of evaporable water left after freeze-drying in the more mature specimens. A third contributing factor might be the dehydration of C–S–H reaction product, as noted by various authors [27,28]. Evidence for such a product was found by SEM and EDX in the CKD–clay specimens but not in the lime–clay specimens.

It should be noted that areas showing C–S–H (such as the area marked A in Fig. 13) were not common even in the CKD–clay specimens, but such areas may be under-represented on fractures surfaces, which would tend to pass through weaker residual clay.

From the first day of curing, the CKD-treated clay exhibited much stronger and sharper XRD basal peaks than the original clay. Presumably, this reflects a more uniform stacking of the clay unit layers within individual particles, perhaps associated with ion exchange of calcium for sodium (Ca-montmorillonite generally shows better packing). The agglomeration of the clay particles, evident on SEM examination, may be in part, due to this ion exchange, but it also likely reflects the effect of the high ionic strength developed in the clay–water system by the addition of the CKD.

It should be noted that the disappearance of calcium hydroxide, the sharpening of the basal XRD peak for montmorillonite, and the modification of the morphology were all also evident in lime-treated Na-m clay. Thus they seem to be consequences of the interaction of calcium hydroxide present in the hydrated CKD.

Several other features found in the CKD-treated clay were not observed in the lime-treated clay, including the presence of significant (although transient) gypsum contents at early ages, and the production of a small amount of ettringite at later stages. It should be noted that in some systems ettringite may act as a reinforcing component that contributes to initial strength and stiffness; however, progressive formation of ettringite in stabilized clays may result in expansion and induce long term durability issues.

Based on these observations we propose the following mechanism for the observed stabilization of the Na-m clay treated with this CKD:

1) Addition of this CKD to the clay quickly raises the pH to ~13. This high pH is indicative of an OH^- ion activity considerably greater than that induced in the lime treated clay, whose pH is limited to 12.5. While it exists, this high pH creates favorable conditions for local dissolution of clay at surfaces and edges, likely releasing alumina and silica into the solution.
2) The free lime in the CKD hydrates rapidly to form $Ca(OH)_2$, but the $Ca(OH)_2$ is extensively adsorbed by the clay and its existence as an identifiable separate phase ceases after brief curing.
3) The high ionic strength induced by the CKD in the limited amount of available water in the compacted CKD–clay system (and possible ion exchange of calcium for sodium ions) promote rapid agglomeration of the clay. As a result, the morphology of the clay seen in the fracture surface of the CKD-treated clay is substantially different from that seen in the same clay compacted with water alone.
4) Gypsum is formed from the sulfate-bearing components present in the CKD, and subsequently a substantial amount of ettringite is shown to be produced. It seems likely that the latter incorporates some aluminum dissolved from the clay.
5) As curing proceeds, areas of dense C–S–H (or a C–S–H-like phase) is formed in some locations, presumably by pozzolanic reaction of adsorbed $Ca(OH)_2$ with silica (from the clay).

5. Conclusions

Na-montmorillonite, first treated with a particular CKD of high free lime content and then compacted and cured for extended periods, was found to undergo extensive physicochemical changes presumably leading to stabilization and strength development. Calcium hydroxide was initially produced, but it was quickly absorbed by the clay. The bulk clay microstructure revealed by SEM of fractured surfaces underwent considerable modification. The pH of the clay–CKD system was initially elevated to more than 13, but it subsequently dropped to about 12.5 and was maintained at this level despite absence of detectable calcium hydroxide. Some gypsum was produced by the reaction of anhydrite of the CKD with water, and subsequently a substantial amount of ettringite developed, some of the latter presumably incorporating aluminum derived from the clay. C–S–H reaction products, presumably formed by reaction of adsorbed calcium hydroxide with silica from the clay were identified locally on fracture surfaces of the CKD–clay system.

Acknowledgments

The authors thank Dr. Laurent Barceló and Oscar Tavares of Lafarge North America for helpful discussions and for providing the CKD materials and the analyses quoted in Table 1. The assistance of Janet Lovell and of Debbie Sherman at Purdue University is gratefully acknowledged.

References

[1] W.J. McCoy, R.W. Kriner, Use of Waste Kiln Dust for Soil Consolidation, Lehigh Portland Cement Co., Allentown, Pennsylvania, U.S.A., 1971.
[2] J.I. Bhatty, Alternative uses of cement kiln dust, R&D Bulletin, vol. 327, Portland Cement Association, Skokie, Illinois, 1995.
[3] M.C. Santagata, A. Bobet, The use of cement kiln dust (CKD) for subgrade stabilization/modification, SPR No. 2575, Purdue University, West Lafayette, Indiana, USA, 2002.
[4] G.A. Miller, M. Zaman, Field and laboratory evaluation of cement kiln dust as a soil stabilizer, Transportation Research Record 1714 (2000) 25–32.
[5] G.A. Miller, S. Azad, Influence of soil type on stabilization with cement kiln dust, Construction and Building Materials 14 (2) (2000) 89–97.
[6] Z.A. Baghdadi, M.A. Rahman, Potential of cement kiln dust for the stabilization of dune sand in highway construction, Building and Environment 25 (4) (1990) 285–289.
[7] J.R. Connor, S. Cotton, P.P. Lear, Chemical stabilization of contaminated soils and sludges using cement and cement by products, Proceedings of the Cement Industry Solutions to Waste Management, Calgary, Alberta, Canada, Oct. 7–9, 1992, pp. 73–97.
[8] M. McKay, J. Emery, Stabilization/solidification of contaminated soils and sludges using cementitious systems, Proceedings of the Cement Industry Solutions to Waste Management, Calgary, Alberta, Canada, Oct. 7–9, 1992, pp. 135–151.
[9] M.S.Y. Bhatty, Properties of blended cements made with Portland cement, cement kiln dust, fly ash and slag, Proceedings of the 8th International Congress on the Chemistry of Cement, Rio de Janeiro, Brazil, Sept. 22–28, 1986, pp. 118–127.
[10] M.L. Wang, V. Ramakrishnan, Evaluation of blended cement, mortar and concrete made from type III cement and kiln dust, Construction and Building Materials 4 (2) (1990) 78–97.
[11] R.J. Detwiler, J.I. Bhatty, S. Bhattacharja, Supplementary cementitious materials for use in blended cements, R&D Bulletin No.112, Portland Cement Association, Skokie, Illinois, 1996.
[12] M.S. Konsta-Gdoutos, S.P. Shah, Synthesis and properties of novel blended cements based on CKD–Slag blends, Cement and Concrete Research (33) (2003) 269–276.
[13] K. Wang, M.S. Konsta-Gdoutos, S.P. Shah, Hydration, rheology and strength of OPC–CKD–Slag binders, ACI Materials Journal 99 (2) (2002) 173–179.

[14] F.F. Udoeyo, A. Hyee, Strength of cement kiln dust concrete, ASCE Journal of Materials in Civil Engineering (Nov/Dec 2002) 524–526.
[15] A.S. Al-Harthy, R. Taha, F. Al-Maamary, Effect of cement kiln dust (CKD) on mortar and concrete mixtures, Construction and Building Materials 17 (2003) 353–360.
[16] G.J. Hawkins, J.I. Bhatty, A.T. O'Hare, Cement kiln dust production, management and disposal, R&D Serial No.2327, Portland Cement Association, Skokie, Illinois, 2003.
[17] B. Ballivy, J. Rouis, D. Breton, Use of cement residual kiln dust as landfill liner, Proceedings of the Cement Industry Solutions to Waste Management, Calgary, Alberta, Canada, Oct. 7–9, 1992, pp. 99–118.
[18] M.L. Preston, Use of cement kiln dust as an agricultural lime and fertilizer, Emerging Technologies Symposium on Cement and Concrete in the Global Environment, Chicago, March 10–11, Portland Cement Association, Skokie, Illinois, 1993, PCA's Cement Technical Support Library DVD020.01©2005.
[19] S. Peethamparan, J. Olek, K.E. Helfrich, Evaluation of the engineering properties of cement kiln dust (CKD) modified kaolinite clay, Proceedings of the 21st International Conference on Solid Waste Technology and Management, March 26–29, Widener University, Philadelphia, PA, 2006, pp. 997–1006.
[20] S. Peethamparan, J. Olek, A study on the effectiveness of cement kiln dusts (CKDs) in stabilizing Na-montmorillonite clay, ASCE Journal of Materials in Civil Engineering 20 (2) (2008) 137–146.
[21] S. Peethamparan, J. Olek, S. Diamond, Physicochemical behavior of cement kiln dust treated kaolinite clay, Journal of Transportation Research Record — Geomaterials 2059 (2008) 80–88.
[22] S. Diamond, E.B. Kinter, Mechanism of soil–lime stabilization, an interpretive review, Highway Research Record 92 (1965) 83–96.
[23] J.R. Prusinski, S. Bhattacharja, Effectiveness of Portland cement and lime in stabilizing clay soils, Transportation Research Record 1 (1652) (1999) 215–227.
[24] S. Peethamparan, J. Olek, J. Lovell, Influence of chemical and physical characteristics of cement kiln dusts (CKDs) on their hydration behavior and potential suitability for soil stabilization, Cement and Concrete Research 38 (2008) 803–815.
[25] D.L. Sparks, Environmental Soil Chemistry, Elsevier Science (U.S.A.), San Diego, California, 2003.
[26] USBR-5510, Performing Laboratory Compaction of Soils—Harvard Miniature, United States Department of the Interior Bureau of Reclamation, Denver, Colorado, 1989.
[27] J. Dwecka, P.M. Buchler, A.C.V. Coelho, F.K. Cartledge, Hydration of a Portland cement blended with calcium carbonate, Thermochemica Acta 346 (2000) 105–113.
[28] W. Sha, E.A. O'Neill, Z. Guo, Differential scanning calorimetry study of ordinary Portland cement, Cement and Concrete Research 29 (1999) 1487–1489.